Probabilistic analyses of a strip footing on horizontally stratified sandy deposit using advanced constitutive model

R. Suchomel and D. Mašín[1]

Charles University in Prague
Faculty of Science
Albertov 6
12843 Prague 2, Czech Republic
E-mail: masin@natur.cuni.cz
Tel: +420-2-2195 1552, Fax: +420-2-2195 1556

January 6, 2011

Submitted to Computers and Geotechnics

[1]corresponding author

1 Abstract

An advanced hypoplastic constitutive model is used in probabilistic analyses of a typical geotechnical problem, strip footing. Spatial variability of soil parameters, rather than state variables, is considered in the study. The model, including horizontal and vertical correlation lengths, was calibrated using a comprehensive set of experimental data on sand from horizontally stratified deposit. Some parameters followed normal, whereas other followed lognormal distributions. Monte-Carlo simulations revealed that the foundation displacement u_y for a given load followed closely the lognormal distribution, even though some model parameters were distributed normally. Correlation length in the vertical direction θ_v was varied in the simulation. The case of infinite correlation length was used for evaluation of different approximate probabilistic methods (first order second moment method and several point estimate methods). In the random field Monte-Carlo analyses with finite θ_v, the vertical correlation length was found to have minor effect on the mean value of u_y, but significant effect on its standard deviation. As expected, it decreased with decreasing θ_v due to spatial averaging of soil properties.

Key Words: Probabilistic methods; constitutive models; random fields; foundation settlement

2 Introduction

Parameters of simple constitutive models, which are typically used in probabilistic analyses of geotechnical problems, are dependent on the soil state. These models thus do not allow us to distinguish whether the measured variability of soil properties is caused by the variability of soil type or soil state. Contrary to this, advanced constitutive models adopt soil parameters that are specific to the given soil granulometry and mineralogical composition of soil particles. State variables (such as void ratio e) then incorporate the state-dependency of the soil behaviour. In this respect, the sources of the objective (aleatory [25]) uncertainty in soil mechanical behaviour can be subdivided into two groups:

1. In some situations, soil mineralogy and granulometry may be regarded as spatially invariable, and the uncertainty in the mechanical properties of soil deposit come from variability in the soil state. In this case, soil *parameters* of advanced models may be considered as constants, and in the analyses it is sufficient to consider spatial variability of *state variables* describing the relative density of soil.

2. In other cases, soil properties are variable due to varying granulometry and mineralogy of soil grains. Such a situation is for example typical for soil deposits of sedimentary basins, where

the granulometry varies due to the variable geological conditions during the deposition. In such a case, it is necessary to consider spatially variable soil *parameters* in the simulations.

Application of advanced constitutive models within probabilistic numerical analyses still remains relatively uncommon in the geotechnical scientific literature. Moreover, most of the applications of probabilistic methods in combination with advanced soil constitutive models consider the uncertainty in the state variable only, while keeping constant values of the model parameters. As an example, Hicks and Onisiphorou [27] studied stability of underwater sandfill berms. Their aim was to study whether presence of 'pockets' of liquifiable material may be enough to cause instability in a predominantly dilative fill. They used a double-hardening constitutive model Monot [33] with probabilistic distribution of the Been and Jefferies state variable ψ [3]. As the aim of the research was to study whether pockets of loose material may cause failure of the berm, the approach chosen (variation in the state variable only) is fully justifiable. In other applications, Tejchman [45] studied the influence of the fluctuation of void ratio on formation of the shear zone in the biaxial specimen using the hypoplastic model by von Wolffersdorff [47]. Similar procedure and the same constitutive model was used by other researchers in finite element simulations of different geotechnical problems [34, 36]. Finally, Andrade et al. [1] considered random porosity fields in combination with an advanced constitutive model and studied their influence on strength and shear band formation in a biaxial specimen.

The goal of this paper is to present a complete evaluation of the influence of parameter variability of an advanced constitutive model and its influence on predictions of a typical geotechnical problem. To utilise the advantage of the non-linear formulation of the constitutive model adopted, we study settlement of a rigid strip foundation subjected to a given load. While most application of probabilistic methods to the foundation problems focus on the evaluation of the bearing capacity [17, 15, 7, 11, 28, 29, 21, 13], less attention is payed to the quantification of the uncertainty in serviceability limit states. In the available studies, the authors focus on different aspects of the problem, such as foundation size and geometry [30], uncertainty in the foundation load [5], 3D effects [19, 14], differential settlement issues between two footings [12, 14, 34], cross-correlation between elastic parameters E and ν [35], the effects of layers of different materials in the subsoil [32], and comparison with simpler probabilistic methods (such as the first order second moment method) [20]. In many publications, the authors address the influence of the correlation length [35, 14, 19, 12]. In most of these works, however, the soil is modelled as a linear elastic material (or elastic material with stress-dependent Young modulus [30]). An exception is the contribution by Niemunis et al. [34], who used non-linear hypoplastic model with constant parameters and random fields of void ratio in the cyclic analyses of two adjacent strip footings. Most of the available studies thus do not consider the non-linear soil behaviour, which is important for correct predictions of foundation displacements. This issue is addressed in the present work.

3 Experimental program

The material for the investigation comes from the south part of upper Cretaceous Třeboň basin in south Bohemia (Czech Republic) from the sand pit Kolný [42]. The pit is located in the upper part of the so-called Klikovské layers, youngest (senon) strata of the south Bohemian basins. These fluvial layers are characterised by a rhythmical variation of gravely sands, sands and clayey sands.

Altogether forty samples were obtained from a ten meters high pit wall in a regular rectangular grid (Fig. 1). The laboratory program was designed to provide for each of the samples enough

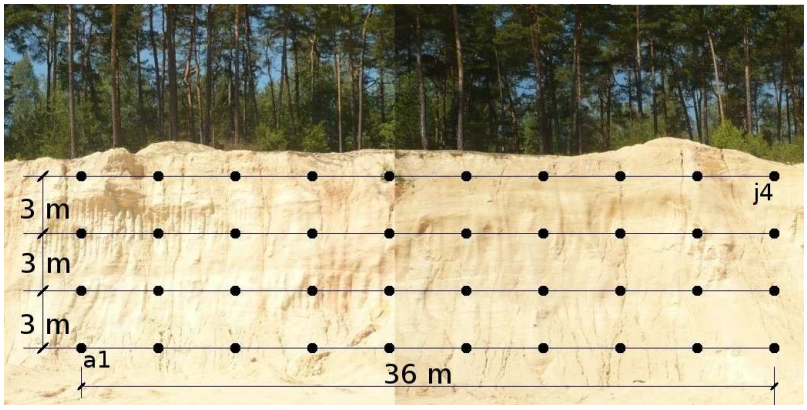

Figure 1: The wall of the sand pit in south part of the Třeboň basin. Black dots represent positions of specimens for the laboratory investigation.

information to calibrate the hypoplastic model for granular materials by von Wolffersdorff [47]. The following tests were performed on each of the 40 samples:

- Oedometric compression tests on initially very loose specimens with loading steps 100, 200, 400, 800, 1600, 3200 and 6400 kPa.
- Drained triaxial compression test on specimen dynamically compacted to void ratio corresponding to the dense *in-situ* conditions. One test per specimen at the cell pressure of 200 kPa.
- Measurement of the angle of repose.

Results of all the laboratory experiments are presented in the Appendix. Location of the specimens, labeled as $a1$ to $j4$, is indicated in Fig. 1. Note that 4 specimens ($c1$, $e4$, $f1$, $f2$) showed unusual behaviour, and these specimens were not used in the evaluation.

In addition to laboratory experiments, five *in-situ* porosity tests with membrane porosimeter were performed at different locations within the area from which the samples were obtained. Average natural void ratio was 0.41. The porosity was found to be fairly uniform and the sand was in very dense conditions. Note that the triaxial tests were not performed at the initial void ratio exactly corresponding to the in-situ conditions, as this was not known for each of the 40 samples. This fact should, however, not influence the model calibration, as parameters of advanced hypoplastic models depend on soil type and granulometry only, and do not significantly depend on its state [26, 24].

4 Calibration of hypoplastic constitutive model

The constitutive model selected for this research work is based on hypoplasticity, a particular class of incrementally nonlinear constitutive models. The hypoplastic equation may be written as

$$\mathring{\mathbf{T}} = f_s \boldsymbol{\mathcal{L}} : \mathbf{D} + f_s f_d \mathbf{N} \|\mathbf{D}\|. \tag{1}$$

where $\mathring{\mathbf{T}}$ is the objective (Jaumann) stress rate, $\mathbf{D}$ is the Euler's stretching tensor and $\boldsymbol{\mathcal{L}}$ and $\mathbf{N}$ are fourth- and second order constitutive tensors, respectively. f_s and f_d are scalar factors expressing the influence of the stress level (barotropy) and density (pyknotropy). The model adopted in this research was proposed by von Wolffersdorff [47] based on the earlier work of the Karlsruhe research group (e.g., [31, 22, 2]). For an interpretation of the model response see [23].

The hypoplastic model by von Wolffersdorff [47] has eight material parameters, namely φ_c, h_s, n, e_{d0}, e_{c0}, e_{i0}, α and β. Their calibration procedure was detailed by Herle and Gudehus [26]. A somewhat simplified calibration procedure has been adopted in the present work. The whole process of calibration has been automated to reduce subjectivity of calibration.

The critical state friction angle φ_c has been obtained directly by the measurement of the angle of repose. The hypoplastic model considers that the soil state in the e vs. p space is bound by maximum (e_i) and minimum (e_d) void ratios, as shown in Fig. 2. In addition, critical state line in the e vs. p space is characterised by void ratio e_c. The three curves are described by formula due to Bauer [2]

$$\frac{e_c}{e_{c0}} = \frac{e_d}{e_{d0}} = \frac{e_i}{e_{i0}} = \exp\left[-\left(\frac{3p}{h_s}\right)^n\right] \tag{2}$$

with five parameters. The parameter n controls the curvature of the curves and h_s controls the overall slope of the curves. The parameters e_{d0}, e_{c0} and e_{i0} control their positions (they represent the values of the reference void ratios for $p = 0$ kPa).

The parameters h_s and n were directly computed from oedometric loading curves in the interval of

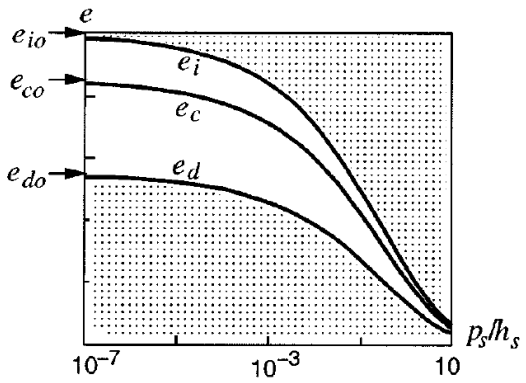

Figure 2: The dependency of the reference void ratios e_d, e_c and e_i on the mean stress (Herle and Gudehus [26]).

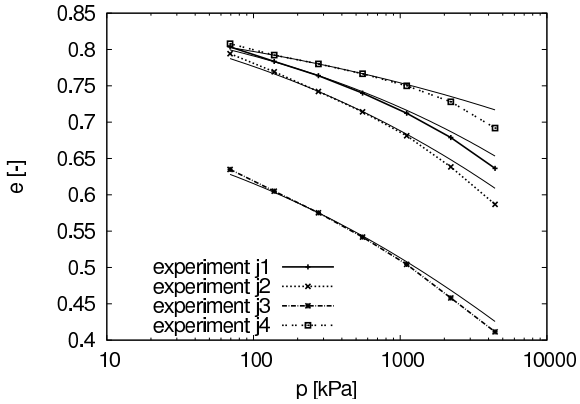

Figure 3: Computed curves using h_s, n, e_{c0} parameters for one column of specimens.

$\sigma_a \in \langle 100, 1000 \rangle$ kPa using procedure detailed in [26]. Following Herle and Gudehus [26], initial void ratio e_{max} of a loose oedometric specimen was considered equal to the critical state void ratio at zero pressure e_{c0}. Figure 3 shows comparison of compression curves calculated using formula by Bauer (2) with compression curves obtained from the oedometric test (for illustration purposes specimens from one column of the sampling grid only).

Void ratios e_{d0} and e_{i0} were obtained from empirical relations. The physical meaning of e_{d0} is the reference void ratio at maximum density, whereas void ratio e_{i0} represents the intercept of the isotropic normal compression line with $p = 0$ axis. Void ratio e_{i0} was obtained by multiplying e_{c0} by a factor 1.2 [26]. The minimum void ratio e_{d0} was also calculated from e_{c0}. e_{c0} was multiplied by a factor 0.379. This ensured that the initial void ratio for triaxial specimens was always higher than e_d and the initial state was close to the state of maximum density. The state thus corresponded

to the dense *in-situ* conditions.

The last two parameters of the hypoplastic model α and β control independently different aspects of soil behaviour. Namely, the parameter β controls the shear stiffness and α controls peak friction angle. They were calibrated by single-element simulations of the drained triaxial tests. Fig. 4 shows comparison of typical experimental and simulated q vs. ϵ_a and ϵ_v vs. ϵ_s curves (specimens from one column of the sampling grid only). The hypoplastic model calibrated using the outlined procedures reproduced closely the q vs. ϵ_a curves. It somewhat underestimated the initial rate of dilatancy.

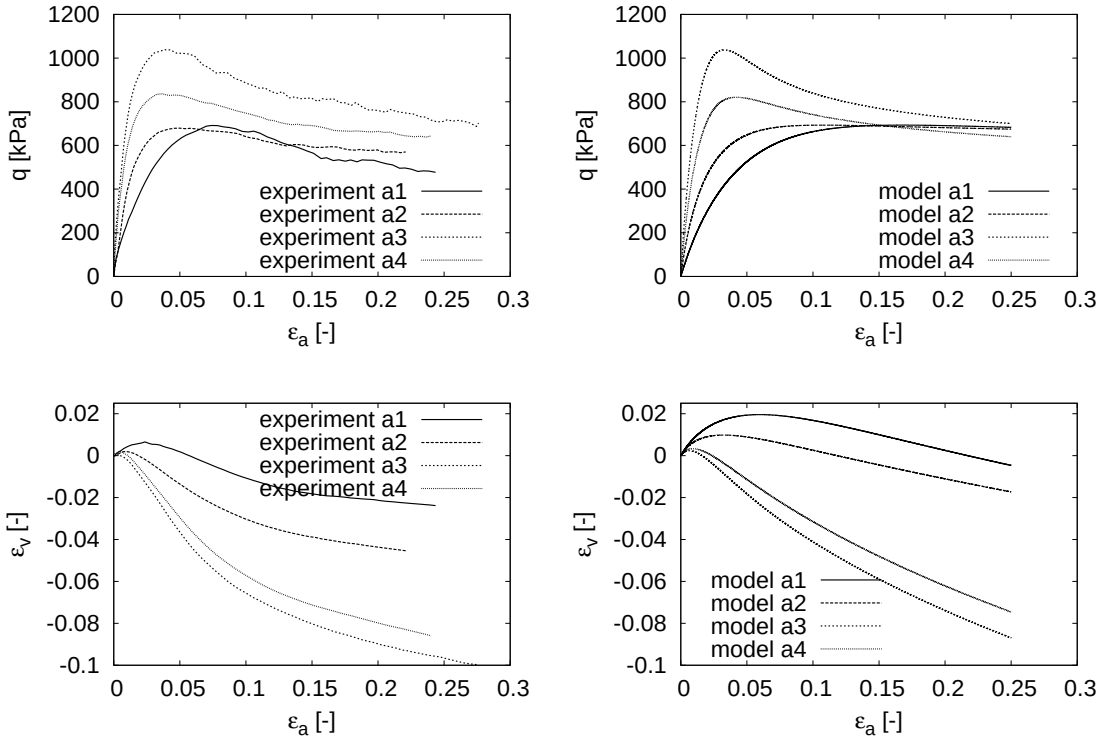

Figure 4: Typical experimental and simulated results of drained triaxial tests.

5 Probabilistic distribution of the model parameters and correlation properties

Statistical distribution of the parameters calibrated using experiments described in Sec. 3 is shown in Fig. 5. Parameters e_{i0} and e_{d0} of the hypoplastic model are not presented in Fig. 5 as they are multiples of the value of e_{c0}. For each parameter, suitability of normal and log-normal distributions to represent the experimental data was studied using Kolmogorov-Smirnov and χ^2 tests. More

suitable distribution and its characteristic values are indicated in Tab. 1. These values were used in all subsequent simulations.

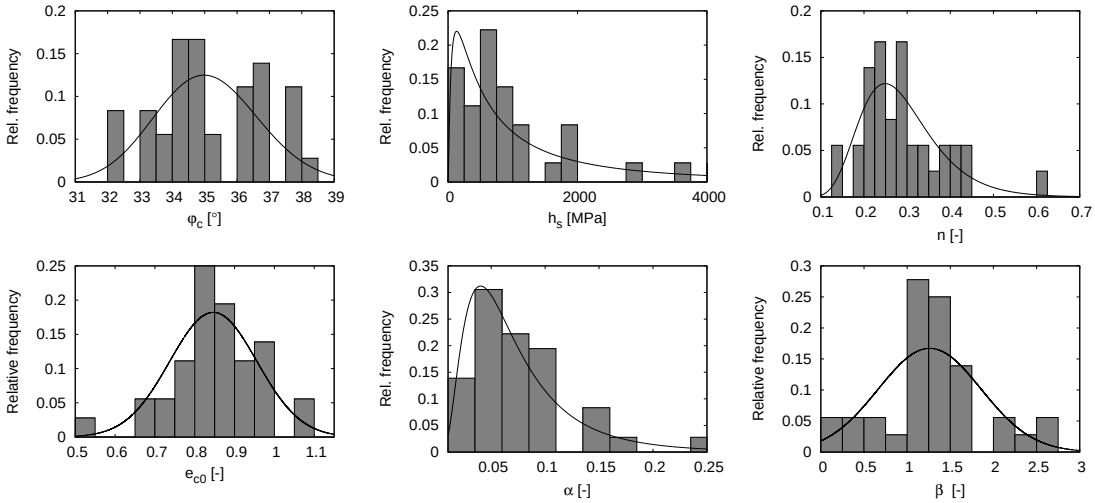

Figure 5: Statistical distributions of hypoplastic parameters.

5.1 Cross-correlation of parameters

The correlation coefficient $\rho_{X,Y}$ between two variables X and Y is defined as

$$\rho_{X,Y} = \frac{E\left[(X-\mu_X)(Y-\mu_Y)\right]}{\sigma[X]\sigma[Y]} \tag{3}$$

where E is the expected value operator (mean), μ and σ represent mean and standard deviation respectively. Table 2 indicates the correlation coefficient ρ between different parameters for the 36 evaluated specimens. Note that the parameters e_{d0} and e_{i0} are not included in Tab. 2, as they are fully correlated with e_{c0} as a consequence of the adopted calibration procedure.

Table 2 shows that the cross-correlation between the parameters is rather poor, with the exception of negative correlation between φ_c - α and e_{c0} - α, and positive correlation between β - α. In these cases $|\rho| > 0.5$.

The dependency of these parameter pairs is given in Fig. 6. Although some dependency is evident, it is considered not to be significant to influence remarkably the results of finite element simulations. For this reason, no cross-correlation of parameters has been considered in the simulations. An exception are the parameters e_{c0}, e_{d0} and e_{i0}, which have been considered as fully correlated due to the reasons explained above.

Table 1: Characteristic values of statistical distributions of parameters of the hypoplastic model (”norm.” for Gaussian distribution, ”log” for log-normal distribution) .

param.	dist.	mean	st. dev.
φ_c	log.	35.1°	1.62°
h_s	log.	3.82 GPa	14.6 GPa
n	log.	0.289	0.095
e_{c0}	norm.	0.847	0.111
e_{i0}	norm.	1.016	0.133
e_{d0}	norm.	0.318	0.042
α	log.	0.074	0.048
β	norm.	1.261	0.605

Table 2: Cross-correlation of the model parameters.

param.	φ_c	h_s	n	e_{c0}	α	β
φ_c	1.00	-0.27	0.19	0.16	-0.51	-0.23
h_s		1.00	-0.24	0.13	0.05	-0.23
n			1.00	-0.20	-0.16	-0.25
e_c				1.00	-0.71	-0.42
α					1.00	0.60
β						1.00

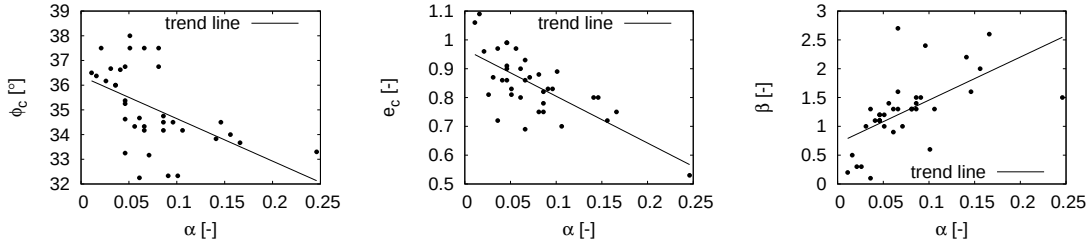

Figure 6: Cross-correlation between parameter pairs φ_c - α, e_c - α, β - α.

5.2 Spatial correlation of parameters

In addition to the cross-correlation between different parameters, complete probabilistic description of the soil deposit requires specification of the spatial auto-correlation of the parameters, i.e. the dependency of the correlation coefficient of given parameter on distance. This dependency is commonly approximated using expression due to Markov

$$\rho = \exp\left[-2\sqrt{\left(\frac{\tau_h}{\theta_h}\right)^2 + \left(\frac{\tau_v}{\theta_v}\right)^2}\right] \tag{4}$$

where τ_h is the horizontal distance between two specimens, τ_v is the vertical distance and θ_h and θ_v are so-called correlation lengths in horizontal and vertical directions respectively [46]. These describe a distance upon which the parameters are significantly correlated.

The correlation lengths could successfully be evaluated using parameter φ_c only. This parameter depends directly on soil granulometry. The least square fit of Eq. (4) through the experimental data is shown in Figure 7, leading to $\theta_h = 242$ m and $\theta_v = 5.1$ m.

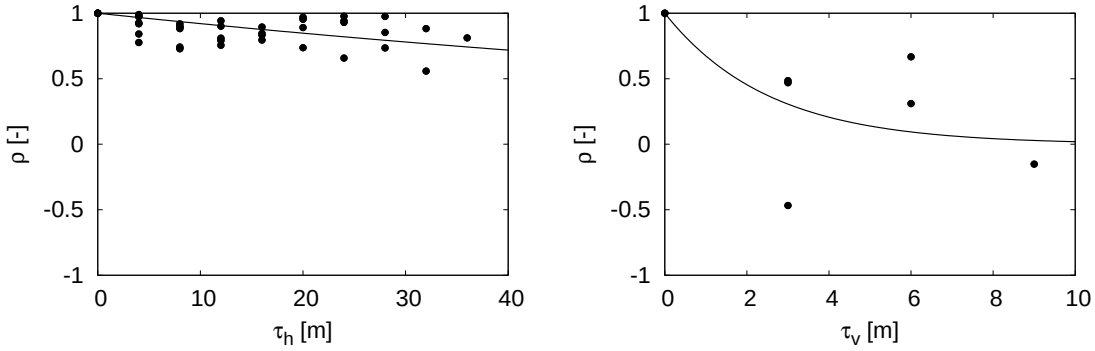

Figure 7: Evaluation of the correlation coefficient ρ in horizontal (a) and vertical (b) directions for parameter φ_c, together with least square fit of Eq. (4).

Note that using the 40 samples described in Sec. 3, practically no correlation is observed in the vertical direction. The obtained value $\theta_v = 5.1$ m is thus implied by the adopted vertical sampling distance only, rather than by the actual autocorrelation properties. For this reason, additional sampling and experimental programme was devised. In the additional experiments, only the critical state friction angle φ_c (angle of repose) was studied. The vertical sampling distance was 0.05 m, and the soil profile was 5 m high. The location of the studied profile was within the same quarry wall as the profile used for extraction of the 40 specimens from Sec. 3.

Results of measurements are shown in Fig. 8, altogether with a detailed view of the profile. The

measurements are highly scattered. Nonetheless, an attempt has been made to distinguish zones of different average friction angles (shown as bold lines in Fig. 7). Average length of these zones was used as an approximation of the vertical correlation length, leading to $\theta_v = 0.31$ m. Figure 8 also shows random field (see Sec. 8.3) of φ_c, generated with parameters from Tab. 1 and $\theta_v = 0.31$ m and $\theta_h = 242$ m. The generated profile approximates well the measured distribution of φ_c and the observed layered structure of the soil deposit.

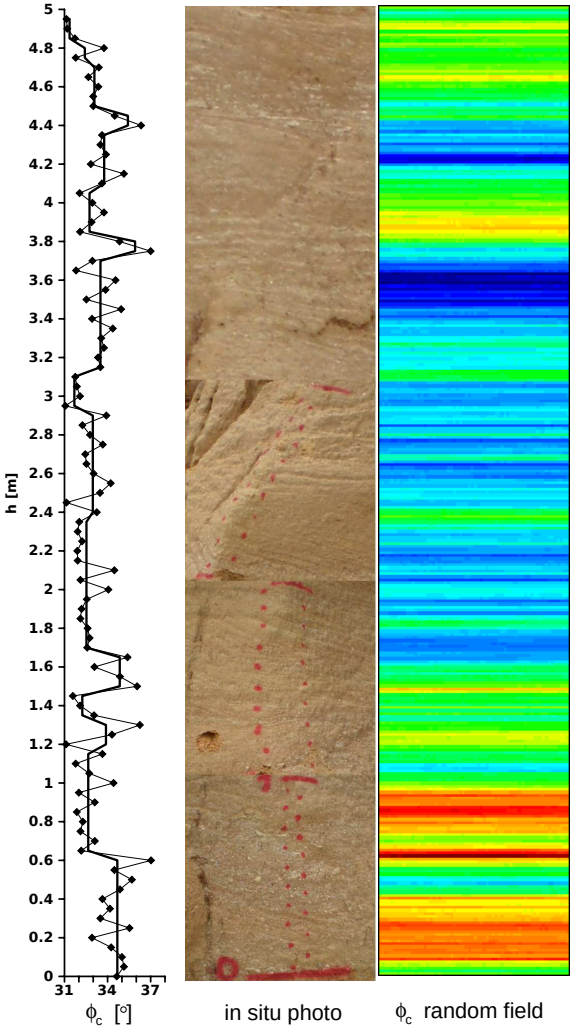

Figure 8: Evaluation of the vertical correlation length using detailed measurements of φ_c. Random field for $\theta_v = 0.31$ m.

6 Strip footing problem

The influence of spatial variation of parameters of the hypoplastic model was studied by simulations of a typical geotechnical problem – settlement of a strip footing [44]. Simulations were performed using a finite element package *Tochnog Professional* [38]. The individual simulations were deterministic. Probabilistic aspects were introduced in Sec. 8 by variation of the input material parameters and evaluation of the simulations outputs.

The problem geometry and the finite element mesh for most analyses are shown in Figure 9. The mesh consisted of 1920 nine-noded quadrilateral elements. The foundation was analysed as rigid and perfectly smooth. Element size in the vicinity of the footing was 0.5 m. The adopted mesh density was found to be sufficient for all analyses, except of random field analyses (Sec. 8.3) with $\theta_v = 0.31$ m. In these analyses, four-times denser mesh was used (7680 nine-noded quadrilateral elements with the element size in the vicinity of the footing equal to 0.25 m).

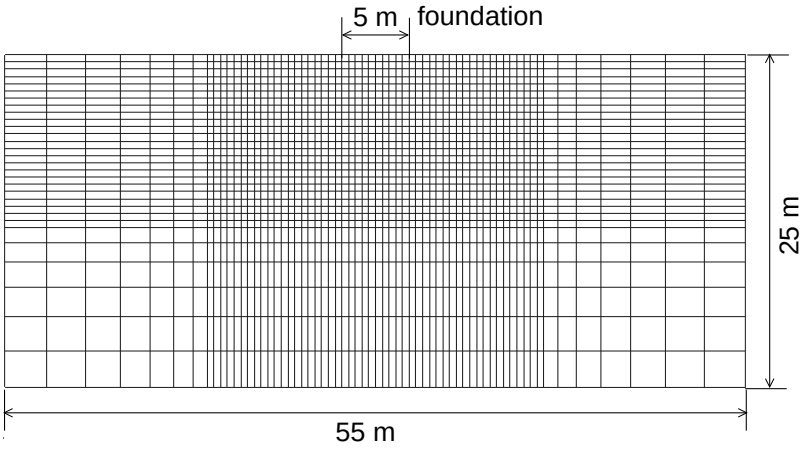

Figure 9: The problem geometry and finite element mesh for $\theta_v \geq 1$ m. Four times denser mesh used in analyses with $\theta_v = 0.31$ m.

The soil unit weight was 18.7 kN/m^3. The initial $K_0 = 0.43$ was calculated from Jáky formula $K_0 = 1 - \sin\varphi_c$, with average value of φ_c measured in the experiments. The initial value of void ratio $e = 0.48$ was used in simulations. The simulated soil was thus slightly looser than measured *in situ*. In this way, it was ensured that the statistical distribution of e_d did not have to be truncated due to $e < e_d$ (such a state is inallowed in hypoplasticity). Trunctation of the statistical distribution would complicate subsequent evaluation of simpler probabilistic methods (Sec. 8.2). Spatial variability of void ratio was not considered. The analyses thus focused on the evaluation of the influence of the spatial variability of soil parameters. In all the cases, foundation displacements corresponding to the load of 500 kPa were evaluated.

7 Sensitivity analysis

First, sensitivity of the results on different material parameters was evaluated. The subsequent probabilistic analyses from Sec. 8 then focused on the most influencial parameters in the evaluation of the influence of the parameter uncertainty. In sensitivity analyses, the problem was for each of the parameters simulated three times - using the mean values of the parameters, and for $\mu[X] \pm \sigma[X]$. X stands for a parameter value in the case of normally distributed parameters and its logarithm in the case of lognormally distributed parameters. Only one parameter was varied at a time, all other parameters were given their mean or median values (for normally and lognormally distributed parameters respectively). The results were graphically represented using so-called "tornado diagram" (Fig. 10).

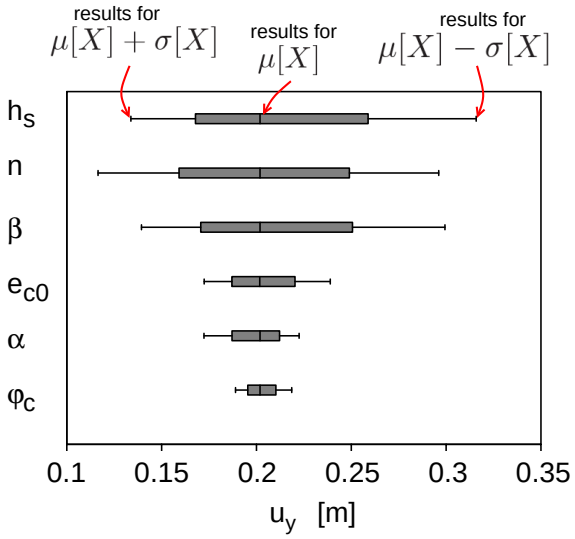

Figure 10: Tornado diagram showing sensitivity of foundation displacements on different parameters.

As expected, foundation settlements are influenced most significantly by the parameters controlling soil bulk modulus (parameters h_s and n). They are followed by the parameter β, which influences the shear stiffness. Less significant is the influence of the relative density, controlled through parameters e_{c0}, e_{i0} and e_{d0}. Note that e_{c0} and the other two reference void ratios e_{i0} and e_{d0} were varied simultaneously to ensure constant ratios between them imposed during calibration (Sec. 4). Parameters α and φ_c have the smallest influence on foundation settlements. These parameters control the soil strength, rather then stiffness, and their minor influence on pre-failure foundation settlements is thus a reasonable observation.

8 Probabilistic analyses

In the analysis of uncertain systems, the uncertainty of the input variables is propagated through the system leading to the assesment of uncertainty of its response [41]. The strip footing problem in scope of this study can be for the *given parameter set* considered as deterministic. Such a problem can be solved using probabilistic numerical methods. The probabilistic characteristics of the problem are studied by variation of the input parameters and evaluation of the simulation output.

The following probabilistic methods have been evaluated in the present work. First of all, the strip footing problem has been simulated without considering spatial variability of the parameters (i.e. with infinite correlation length) using a fully general Monte-Carlo method. These results serve as a benchmark for the simulation using approximate probabilistic methods. Then, different approximate analytical probabilistic methods for evaluation of the first two statistical moments of the performance function have been evaluated. These methods are much less computationally demanding, and they are thus more suitable for practical applications provided they give accurate results. Finally, spatial variability of the parameters have been introduced through Monte-Carlo simulations based on random field theory by Vanmarcke [46].

The geotechnical problem of the interest could be, apart from the above mentioned probabilistic methods, solved using more general stochastic numerical analysis. Two main variants of the stochastic finite element method (SFEM) are available in the literature [41]: i) perturbation approach, which is based on a Taylor series expansion of the response vector and ii) the spectral stochastic finite element method, where each response quantity is represented using a series of random Hermite polynomials [16]. In the SFEM methods, the uncertainty is typically treated within the finite element discretisation, and it is thus often not possible to apply the existing deterministic finite element tools without major modifications. Such methods are not readily available to prectitioners as yet. They are thus outside the scope of the present work.

8.1 Monte-Carlo analyses with infinite correlation length

The probabilistic aspects of the problem analysed in this contribution are fairly complex. The constitutive model and thus also the dependency of u_y on the parameter vector $\mathbf{X}$ are non-linear. Some of the model parameters follow Gaussian distributions, whereas other follow lognormal distributions. For this reason, to obtain reference values unbiased by simplifications involved in approximate solutions (Sec. 8.2), analyses with spatially invariable fields of input variables were first performed using Monte-Carlo method. Another reason for running the Monte-Carlo analyses was that the approximate methods do not provide any information on the type of the statistical distribu-

tion of the output variable. They only approximate the first statistical moments (typically the first two moments, i.e. mean and standard deviation). In Monte-Carlo analyses, uniformly distributed random numbers were generated by an unbiased random number generator. Gaussian distributions of the parameters were then obtained by the Box-Muller transformation method [4].

The Monte-Carlo method is fully general, but depending on the problem solved it may require significantly large number of realisations and consequently a considerable computational effort. Figure 11 shows the dependency of the mean value $\mu[u_y]$ and standard deviation $\sigma[u_y]$ for a random field simulation from Sec. 8.3. At least 700 Monte-Carlo realisations is required to get a reasonably stable estimate of $\mu[u_y]$ and $\sigma[u_y]$, depending on the standard deviation of the output variable. In all the presented simulations, at least 1000 realisations were performed.

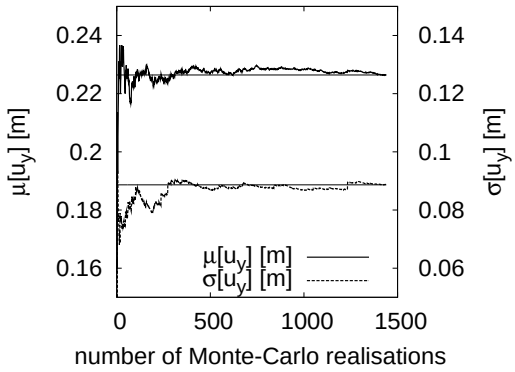

Figure 11: The dependency of $\mu[u_y]$ and $\sigma[u_y]$ on the number of Monte-Carlo realisations (random field simulation with all parameters random and $\theta_v = 5.1$ m).

Four analyses were performed. In three of them, only one parameter was varied at a time and the other parameters were given their mean (normal parameters) or median (lognormal parameters) values. These analyses were performed for the parameters h_s, n and β (the most influential parameters, see Sec. 7). β follows a normal distribution, whereas h_s and n follow lognormal distribution. In the last analysis, all parameters were considered as random.

Figure 12 shows probabilistic distributions of u_y and Tab. 3 gives the values of $\mu[u_y]$ and $\sigma[u_y]$. The distribution of the output variable is well described by the lognormal distribution, even in the case of β as a single variable parameter, which itself follows the Gaussian distribution. Slight deviation from the log-normal distribution show the analyses with n and all parameters random.

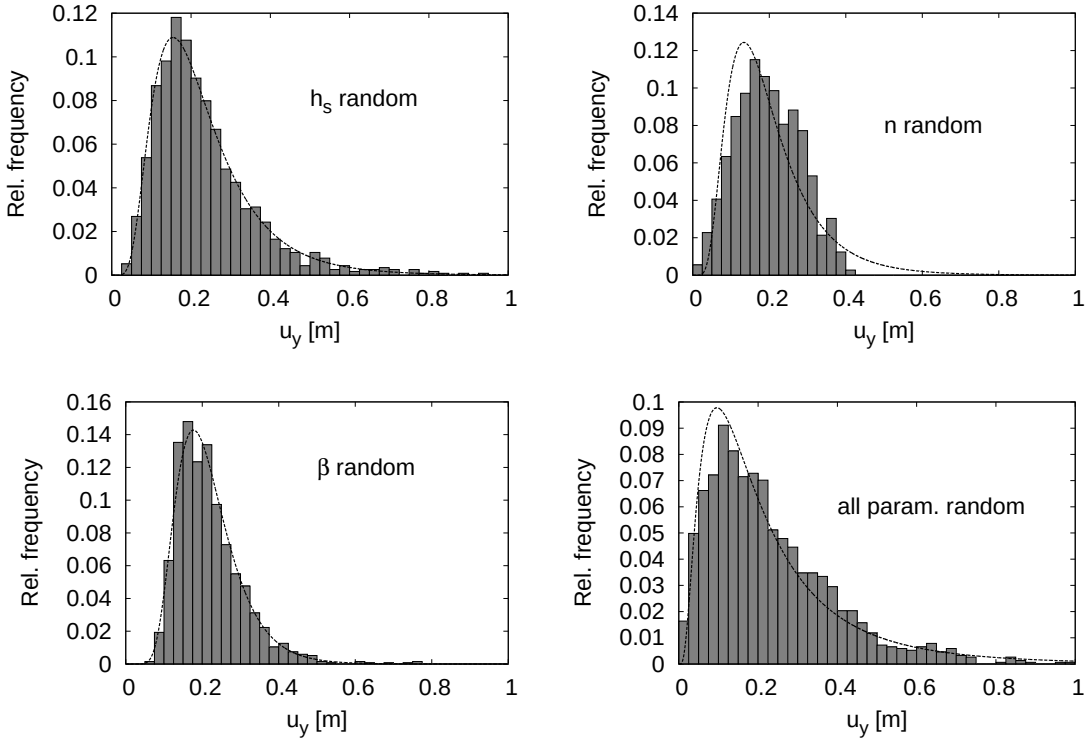

Figure 12: Probabilistic distributions of u_y for Monte-Carlo analyses with infinite correlation length.

Table 3: Results of probabilistic simulations with infinite correlation length ($\mu[u_y]$ and $\sigma[u_y]$ in meters).

method	Monte-Carlo		FOSM		RosPEM		ZNIII	
random param.	$\mu[u_y]$	$\sigma[u_y]$	$\mu[u_y]$	$\sigma[u_y]$	$\mu[u_y]$	$\sigma[u_y]$	$\mu[u_y]$	$\sigma[u_y]$
h_s	0.231	0.128	0.193	0.107	0.225	0.107	0.225	0.127
n	0.197	0.083	0.193	0.089	0.198	0.089	0.197	0.082
β	0.217	0.087	0.193	0.077	0.211	0.077	0.219	0.087
all param.	0.230	0.164	0.193	0.164	0.240	0.170	0.255	0.197

8.2 Simulations with approximate analytical probabilistic methods

The Monte-Carlo method, used in the previous section, is fully general, but requires large number of trials (approx. 1000 in the present case, Fig. 11). This limits its practical applicability. For this reason, approximate approaches to evaluate statistical distribution of the performance function, which require remarkably lower number of simulations, are popular in geotechnical engineering applications. This section is devoted to evaluation of the applicability of several popular methods to simulate the complex non-linear probabilistic problem studied in this paper.

The problem solved may be in general written as $Y = g(X_1, X_2, \ldots, X_n)$, where Y is the performance function (in the present case, $Y = u_y$), and $\mathbf{X} = X_i$ is the vector of random variables (in the present case, $\mathbf{X}$ is the vector of model parameters). Only independent (covariance $Cov[X_i, X_j] = 0$) normal random variables X_i are considered in this work. Log-normal distributions of several parameters were converted to normal distributions by considering their logarithms in the computations. The parameters e_{c0}, e_{d0} and e_{i0} were varied simulatenously so they were treated as a single random parameter.

The first method studied, possibly the most popular in geotechnical engineering, is based on approximating Y by a Taylor series expanded about the expected values of input random variables X_i. Neglecting the second- and higher order terms leads to the following expressions for the first two statistical moments of Y (mean $\mu[Y]$ and standard deviation $\sigma[Y]$):

$$\mu[Y] = g(\mu[X_1], \mu[X_2], ...\mu[X_n]) \tag{5}$$

$$\sigma^2[Y] = \sum_{i=1}^{n} \left(\frac{\partial Y}{\partial X_i} \sigma[X_i] \right)^2 \tag{6}$$

where the partial derivative derivatives $\partial Y / \partial X_i$ are taken at the $\mu[X_i]$. The most common approach uses finite differences for their approximations [9]. Although the derivative at the point is most precisely evaluated using a very small increment of X_i, evaluating the derivative over a range of $\pm\sigma[X_i]$ may according to some authors better capture some of the non-linear behaviour of the function over a range of likely values [48]. Thus, we have

$$\frac{\partial Y}{\partial X_i} = \frac{g\left(\mu[X_i] + \sigma[X_i]\right) - g\left(\mu[X_i] - \sigma[X_i]\right)}{2\sigma[X_i]} \tag{7}$$

Eqs. (5) - (7) describe the so-called first-order (only first-order terms of Taylor series expansion are considered) second-moment (only the first two statistical moments of Y are calculated) method (FOSM). The method requires $2n + 1$ simulations (n is a number of random variables) and it is accurate for performance functions linear in X_i. With increasing non-linearity of Y in X_i, however, omission of the higher order terms of Taylor series expansion and the finite-difference

approximation of $\partial Y/\partial X_i$ leads to an accumulation of an error [6].

In the second class of methods (denoted as point estimate methods, PEM), probability distributions for continuous random variables X_i are replaced by discrete distributions. Each component of the discrete distribution (*point estimate*) is associated with the corresponding weight such that the discrete distribution has the same first few moments as the continuous random variable. Transformation $Y = g(\mathbf{X})$ can be used to calculate the associated discrete distribution of the performance functions, whose moments approximate the moments of Y in the continuous case [8]. This procedure is equivalent to the calculation of the integral of Y using numerical quadrature [8, 49].

A number of point estimate methods is available throughout the literature. In this work, we evaluate the basic method by Rosenblueth [39] (denoted as RosPEM), and more advanced method by Zhou and Nowak [49] (denoted as ZNIII [37, 40]). The RosPEM method requires 2^n simulations, whereas the ZNIII method requires $2n^2 + 1$ simulations. The mean and standard deviation of Y can be obtained from

$$\mu[Y] = \sum_{j=1}^{m} w_j g(\mathbf{X}_j) \tag{8}$$

$$\sigma^2[Y] = \sum_{j=1}^{m} w_j \left(g(\mathbf{X}_j) - \mu[Y]\right)^2 \tag{9}$$

Sample points and corresponding weights for the two evaluated methods are given in Tab. 4 in terms of standard normal variables $\mathbf{Z}$. For normally distributed $\mathbf{X}$ we have $\mathbf{X} = \mu[\mathbf{X}] + \mathbf{Z}\sigma[\mathbf{X}]$.

Table 4: Sample points and corresponding weights for the two evaluated point estimate methods. n is number of random variables.

method	sample points $\mathbf{Z}_j$	weight factors w_j
RosPEM	$\mathbf{Z} = (\pm 1, \pm 1, \cdots \pm 1)^a$	$\dfrac{1}{2^n}$
ZNIII	$\mathbf{Z} = (0, 0, \ldots 0)$	$w = \dfrac{2}{n+2}$
	$\mathbf{Z} = \left(\pm\sqrt{n+2}, 0, \ldots 0\right)^a$	$w = \dfrac{4-n}{2(n+2)^2}$
	$\mathbf{Z} = \left(\pm\sqrt{\dfrac{n+2}{2}}, \pm\sqrt{\dfrac{n+2}{2}}, 0, \ldots 0\right)^a$	$w = \dfrac{1}{(n+2)^2}$

[a] points include all possible permutations of coordinates

The first two statistical moments predicted by the approximate methods from this section have been compared with the reference values from Monte-Carlo simulations (Tab. 3). In the case of single random parameters, the ZNIII method provides very accurate results, both in terms of $\mu[u_y]$ and $\sigma[u_y]$. The ZNIII method is followed by RosPEM and finally by FOSM, which significantly

underpredicts $\mu[u_y]$. A different picture is, however, obtained if all the six independent parameters are varied at the same time. The ZNIII method overpredicts both $\mu[u_y]$ and $\sigma[u_y]$, while the FOSM method underpredicts $\mu[u_y]$ and gives accurate predictions of $\sigma[u_y]$. The most accurate are in this case predictions by the RosPEM method, with modest overprediction of both $\mu[u_y]$ and $\sigma[u_y]$. Incorrect predictions by the most evolved ZNIII method may be explained by the locations of sample points, which are in the ZNIII method dependent on the number of random variables. With a large number of variables involved in the present simulations, the sample points are located far from the mean parameter values (Tab. 4), leading to insufficient representation of the non-linearity of $g(\mathbf{X})$ in the range of the most likely values of $\mathbf{X}$.

8.3 Random field simulations with different vertical correlation lengths

In the next set of analyses, spatial variability of soil parameters as evaluated in Sec. 5.2 was considered. Due to the uncertainty in the evaluation of the vertical correlation length, the analyses were repeated with different values of θ_v. Random fields were generated using method based on the Cholesky decomposition of the correlation matrix (mid-point method [10]). The point statistics of random input variables was transformed through spatial averaging over the element size [46, 18, 43]. All the parameters were considered as random in this case; e_{c0}, e_{d0} and e_{i0} were perfectly correlated and the other parameters were uncorrelated.

Example random fields (parameters h_s and β) for $\theta_v = 0.31$ m are shown in Figure 13. The same figure shows also corresponding distribution of void ratio after 0.8 m of the foundation displacement. Study of this example, as was well as the other simulations not presented here, reveals that the lowest void ratios occur in softer areas characterised by low values of the parameter β. The parameter h_s, which also has a substantial influence on u_y (Sec. 7), affects due to its highly skewed lognormal distribution (Fig. 5) the results in a global way. The parameter β controls the local deformation pattern. Figure 13 also reveals that the hypoplastic model predicts volumetric compaction (decrease of void ratio) in the areas below the foundation, whereas it predicts dilation along the emerging shear zones below the footing.

Statistical distributions of the output variable u_y are shown in Figure 14. In all the studied cases, u_y is well represented by lognormal distribution. This is consistent with the results of Monte-Carlo simulations with spatially invariable parameters (Sec. 8.1).

Figure 15 and Tab. 5 present $\mu[u_y]$ and $\sigma[u_y]$ predicted by the random field simulations with different values of θ_v. One can observe minimum value of $\mu[u_y]$ at $\theta_v = 1$ m. The influence of θ_v on $\mu[u_y]$ is, however, minor. On the other hand, $\sigma[u_y]$ changes with θ_v substantially. The decrease of $\sigma[u_y]$ with θ_v is caused by the spatial averaging [46] of soil properties, leading to the reduction of the effective variance of the input variables and consequently of the performance function. This

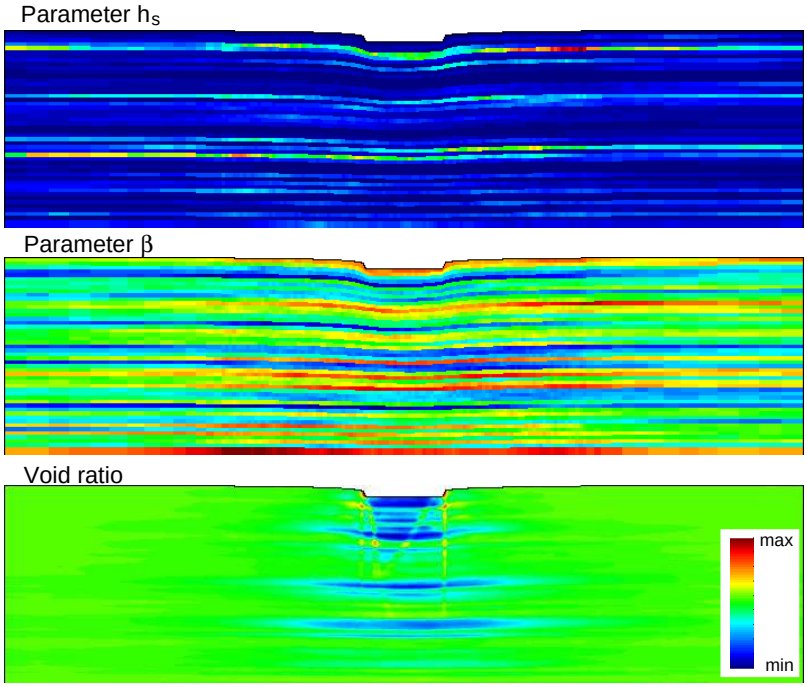

Figure 13: Typical random field simulation with $\theta_v = 0.31$ m (bottom part of the mesh not shown).

issue cannot be captured reliably by simpler probabilistic methods described in Sec. 8.2.

9 Concluding remarks

A comprehensive set of laboratory experiments on stratified sandy deposit was performed in order to calibrate the hypoplastic constitutive model. Some soil parameters followed normal distribution, whereas other followed log-normal distribution. This, altogether with non-linear character of the model, yielded quite a complex problem to be tackled by probabilistic methods. Known positions of different samples enabled us to evaluate spatial correlation of the soil parameters. As expected, due to the horizontally stratified texture of the deposit, the evaluation showed large correlation length in the horizontal direction, and significantly smaller correlation length in the vertical direction. Additional detailed measurements of φ_c yielded an estimate of θ_v as low as 0.31 m.

The model calibrated using the experimental data was subsequently used in probabilistic analyses of a typical geotechnical problem, strip footing. First, the case of infinite correlation length (spatially invariable parameters) was simulated. It was shown that the results were influenced the most by the soil parameters h_s, n and β. Using Monte-Carlo simulations, it was found that the output variable (displacement u_y corresponding to certain footing load) followed a lognormal distribution

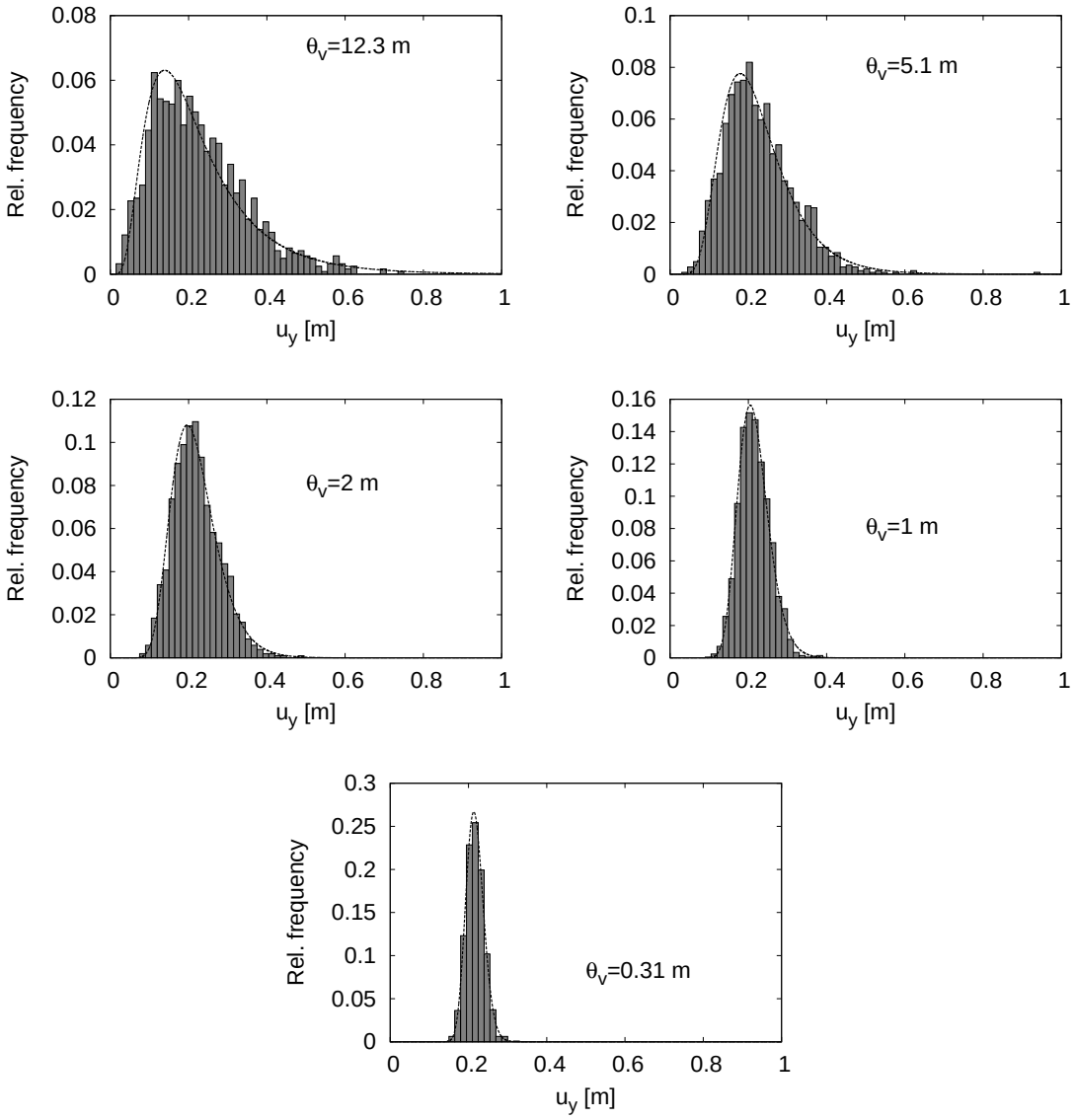

Figure 14: Probabilistic distributions of u_y in random field analyses with different θ_v and all parameters treated as random.

Table 5: Results of Monte-Carlo random field simulations with variable vertical correlation length ($\mu[u_y]$ and $\sigma[u_y]$ in meters).

θ_v	$\mu[u_y]$	$\sigma[u_y]$
∞	0.230	0.164
12.3 m	0.225	0.119
5.1 m	0.226	0.089
2 m	0.219	0.059
1 m	0.215	0.039
0.31 m	0.217	0.023

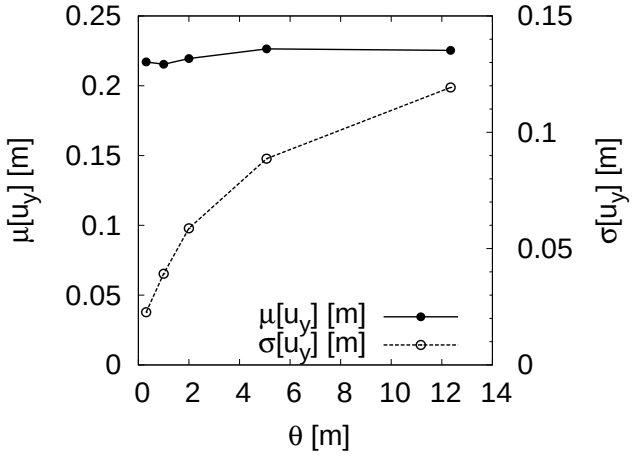

Figure 15: The dependency of $\mu[u_y]$ and $\sigma[u_y]$ on θ_v predicted by the random field method.

closely, even in the case when normally distributed parameters (such as β) were varied. The results of Monte-Carlo analyses were then used for evaluation of different simpler probabilistic methods (the first order second moment method and different point estimate methods). For the complex problem of all parameters treated as random, neither the FOSM method, nor the advanced ZNIII method yielded correct results, for different reasons discussed in the paper. The basic PEM method by Rosenblueth [39] was found the most accurate, although it still overpredicted the mean and standard deviation of u_y. Finally, spatial correlation of the soil parameters was taken into account in Mone-Carlo random field analyses. As expected, spatial averaging of parameters led to a reduction of variance of u_y. This was particularly significant for $\theta_v = 0.31$ m evaluated using detailed measurements of φ_c. The influence of θ_v on the mean value of u_y was minor.

Acknowledgment

The authors wish to thank to Ms. M. Englmaierová and Mr. P. Zmek for performing parts of the experimental programme during their MSc projects. Financial support by the research grants GACR 205/08/0732, GAUK 31109 and MSM 0021620855 is greatly appreciated.

References

[1] J. E. Andrade, J. W. Baker, and K. C. Ellison. Random porosity fields and their influence on the stability of granular media. *International Journal for Numerical and Analytical Methods in Geomechanics*, 32:1147–1172, 2008.

[2] E. Bauer. Calibration of a comprehensive constitutive equation for granular materials. *Soils and Foundations*, 36(1):13–26, 1996.

[3] K. Been and M. G. Jefferies. A state parameter for sands. *Géotechnique*, 35(2):99–112, 1985.

[4] G. E. P. Box and M. E. Muller. A note on the generation of random normal deviates. *Ann. Math. Stat.*, 29:610–611, 1958.

[5] W. Brząkała and W. Puła. A probabilistic analysis of foundation settlements. *Computers and Geotechnics*, 18(4):291–309, 1996.

[6] C.-H. Chang, Y.-K. Tung, and Y. J.-C. Evaluation of probability point estimate methods. *Appl. Math. Modelling*, 19:95–105, 1995.

[7] S. E. Cho and H. C. Park. Effect of spatial variability of cross-correlated soil properties on bearing capacity of strip footing. *International Journal for Numerical and Analytical Methods in Geomechanics*, 34:1–26, 2010.

[8] J. T. Christian and G. B. Baecher. Point-estimate method as numerical quadrature. *Journal of Geotechnical and Geoenvironmental Engineering ASCE*, 125(9):779–786, 1999.

[9] J. T. Christian, C. C. Ladd, and G. B. Baecher. Reliability applied to slope stability analysis. *Journal of Geotechnical Engineering ASCE*, 120(12):2180–2207, 1994.

[10] A. Der Kiureghian and J.-B. Ke. The stochastic finite element method in structural reliability. *Prob Engng Mech*, 3(2):83–91, 1988.

[11] M. D. Evans and D. V. Griffiths. 3D finite analysis of bearing capacity failure in clay. In *Proc. 16^{th} Int. Conf. Soil Mechanics and Geotechnical Engineering*, volume 2, pages 893–896. Millpress Rotterdam Netherlands, 2006.

[12] G. A. Fenton and D. V. Griffiths. Probabilistic foundation settlement on a spatially random soil. *Journal of Geotechnical and Geoenvironmental Engineering ASCE*, 128(5):381–390, 2002.

[13] G. A. Fenton and D. V. Griffiths. Bearing-capacity prediction of spatially random c-ϕ soils. *Canadian Geotechnical Journal*, 40:64–65, 2003.

[14] G. A. Fenton and D. V. Griffiths. Three-dimensional probabilistic foundation settlement. *Journal of Geotechnical and Geoenvironmental Engineering ASCE*, 131(2):232–239, 2005.

[15] G. A. Fenton, D. V. Griffiths, and X. Zhang. Load and resistance factor design of shallow foundations against bearing failure. *Canadian Geotechnical Journal*, 45:1556–1571, 2008.

[16] R. Ghanem and P. Spanos. *Stochastic Finite Elements: A Spectral Approach*. Springer-Verlag, Berlin, 1991.

[17] D. V. Griffiths and G. A. Fenton. Bearing capacity of spatially random soil: the undrained clay Prandtl problem revisited. *Géotechnique*, 51(4):351–359, 2001.

[18] D. V. Griffiths and G. A. Fenton. Probabilistic slope stability analysis by finite elements. *Journal of Geotechnical and Geoenvironmental Engineering ASCE*, 130(5):507–518, 2004.

[19] D. V. Griffiths and G. A. Fenton. Probabilistic settlement analysis of rectangular footings. In *Proc. 16^{th} Int. Conf. Soil Mechanics and Geotechnical Engineering*, volume 2, pages 1041–1044. Millpress Rotterdam Netherlands, 2006.

[20] D. V. Griffiths and G. A. Fenton. Probabilistic settlement analysis by stochastic and random finite element methods. *Journal of Geotechnical and Geoenvironmental Engineering ASCE*, 135(11):1629–1637, 2009.

[21] D. V. Griffiths, G. A. Fenton, and N. Manoharan. Bearing capacity of rough rigid strip footing on cohesive soil: probabilistic study. *Journal of Geotechnical and Geoenvironmental Engineering ASCE*, 128(9):743–755, 2002.

[22] G. Gudehus. A comprehensive constitutive equation for granular materials. *Soils and Foundations*, 36(1):1–12, 1996.

[23] G. Gudehus and D. Mašín. Graphical representation of constitutive equations. *Géotechnique*, 52(2):147–151, 2009.

[24] V. Hájek, D. Mašín, and J. Boháč. Capability of constitutive models to simulate soils with different OCR using a single set of parameters. *Computers and Geotechnics*, 36(4):655–664, 2009.

[25] J. C. Helton. Uncertainty and sensitivity analysis in the presence of stochastic and subjective uncertainty. *Journal of Statistical Computation and Simulation*, 57:3–76, 1997.

[26] I. Herle and G. Gudehus. Determination of parameters of a hypoplastic constitutive model from properties of grain assemblies. *Mechanics of Cohesive-Frictional Materials*, 4:461–486, 1999.

[27] M. A. Hicks and C. Onisiphorou. Stochastic evaluation of static liquefaction in a predominantly dilative sand fill. *Géotechnique*, 55(2):123–133, 2005.

[28] M. Huber, P. A. Vermeer, and A. Bárdossy. Evaluation of soil variability and its consequences. In T. Benz and S. Nordal, editors, *Proc. 7th European Conference on Numerical Methods in Geomechanics (NUMGE), Trondheim, Norway*, pages 363–368. Taylor & Francis Group, London, 2010.

[29] K. Kasama, Z. K., and A. J. Whittle. Effects of spatial variability of cement-treated soil on undrained bearing capacity. In *Proc. Int. Conference on Numerical Simulation of Construction Processes in Geotechnical Engineering for Urban Environment*, pages 305–313. Bochum, Germany, 2006.

[30] B. S. N. Kim. Probabilistic analysis of settlement for a floating foundation on soft clay. *KSCE Journal of Civil Engineering*, 6(2):235–241, 2002.

[31] D. Kolymbas. Computer-aided design of constitutive laws. *International Journal for Numerical and Analytical Methods in Geomechanics*, 15:593–604, 1991.

[32] Y. L. Kuo, M. B. Jaksa, W. S. Kaggwa, G. A. Fenton, D. V. Griffiths, and J. S. Goldsworthy. Probabilistic analysis of multi-layered soil effects on shallow foundation settlement. In 9^{th} *Australia New Zealand Conference on Geomechanics, Auckland, New Zealand*, volume 2, pages 541–547, 2004.

[33] F. Molenkamp. Elasto-plastic double hardening model Monot. Technical report, LGM Report CO-218595, Delft Geotechnics, 1981.

[34] A. Niemunis, T. Wichtmann, Y. Petryna, and T. Triantafyllidis. Stochastic modelling of settlements due to cyclic loading for soil-structure interaction. In G. Augusti, G. Schuëller, and M. Ciampoli, editors, *Proceedings of the 9th International Conference on Structural Safety and Reliability, ICOSSAR'05, Rome, Italy*. Millpress, Rotterdam, 2005.

[35] A. Nour, A. Slimani, and N. Laouami. Foundation settlement statistics via finite element analysis. *Computers and Geotechnics*, 29:641–672, 2002.

[36] K. Nübel and C. Karcher. FE simulations of granular material with a given frequency distribution of voids as initial condition. *Granular Matter*, 1:105–112, 1998.

[37] G. M. Peschl and H. F. Schweiger. Raliability analysis in geotechnics with finite elements - Comparison of probabilistic, stochastic and fuzzy set methods. In *Proc.* 3^{rd}.

[38] D. Rodemann. *Tochnog Professional user's manual*. http://www.feat.nl, 2008.

[39] E. Rosenblueth. Two-point estimates in probabilities. *Appl. Math. Modelling*, 5(2):329–335, 1981.

[40] H. F. Schweiger and R. Thurner. Basic concepts and applications of point estimate methods in geotechnical engineering. In D. V. Griffiths and G. A. Fenton, editors, *Probabilistic Methods in Geotechnical Engineering*, volume 491 of *CISM International Centre for Mechanical Sciences*, pages 97–112. Springer Vienna, 2007.

[41] G. Stefanou. The stochastic finite element method: Past, present and future. *Comput. Methods Appl. Mech. Engrg.*, 198:1031–1051, 2009.

[42] R. Suchomel and D. Mašín. Calibration of an advanced soil constitutive model for use in probabilistic numerical analysis. In P. et al., editor, *Proc. Int. Symposium on Computational Geomechanics (ComGeo I), Juan-les-Pins, France*, pages 265–274, 2009.

[43] R. Suchomel and D. Mašín. Comparison of different probabilistic methods for predicting stability of a slope in spatially variable c-phi soil. *Computers and Geotechnics*, 37:132–140, 2010.

[44] R. Suchomel and D. Mašín. Spatial variability of soil parameters in an analysis of a strip footing using hypoplastic model. In T. Benz and S. Nordal, editors, *Proc. 7th European Conference on Numerical Methods in Geomechanics (NUMGE), Trondheim, Norway*, pages 383–388. Taylor & Francis Group, London, 2010.

[45] J. Tejchman. Effect of fluctuation of current void ratio on the shear zone formation in granular bodies within micro-polar hypoplasticity. *Computers and Geotechnics*, 33(1):29–46, 2006.

[46] E. H. Vanmarcke. *Random fields: anaylisis and synthesis*. M.I.T. press, Cambridge, Mass., 1983.

[47] P. A. von Wolffersdorff. A hypoplastic relation for granular materials with a predefined limit state surface. *Mechanics of Cohesive-Frictional Materials*, 1:251–271, 1996.

[48] T. F. Wolff. Evaluating the reliability of existing levees. Technical report, U.S. Army Engineer Waterways Experiment Station, Geotechnical Laboratory, Vicksburg, MS, 1994.

[49] J. Zhou and A. S. Nowak. Integration formulas to evaluate functions of random variables. *Structural Safety*, 5:267–284, 1988.

Appendix

The appendix summarises results of the laboratory experiments used for calibration of the constitutive model and evaluation of the correlation properties.

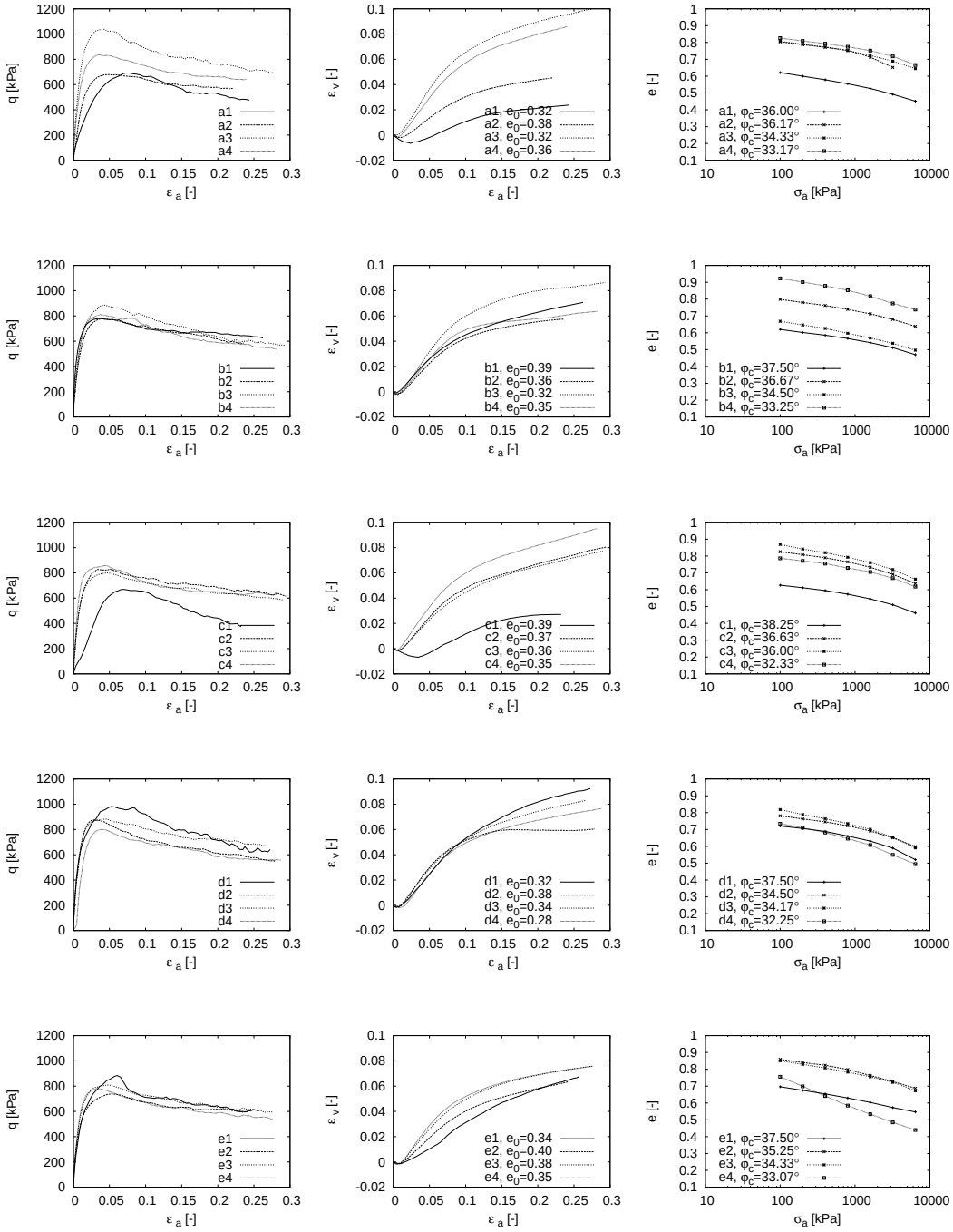

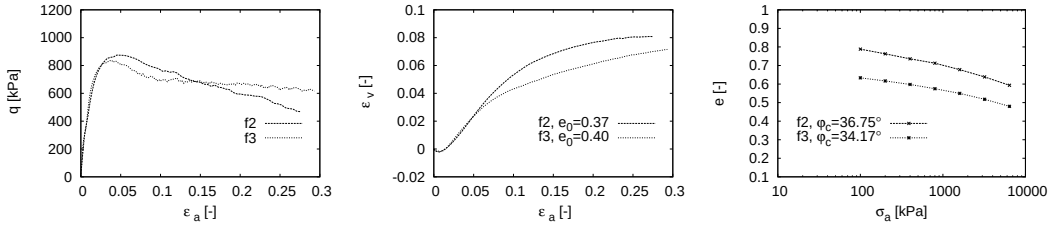
q [kPa]
ε a [-]
f2
f3
ε v [-]
f2, e0=0.37
f3, e0=0.40
e [-]
σa [kPa]
f2, φc=36.75°
f3, φc=34.17°

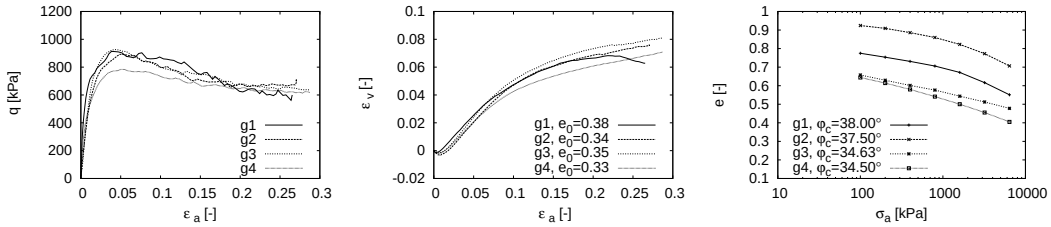
q [kPa]
ε a [-]
g1
g2
g3
g4
ε v [-]
g1, e0=0.38
g2, e0=0.34
g3, e0=0.35
g4, e0=0.33
e [-]
σa [kPa]
g1, φc=38.00°
g2, φc=37.50°
g3, φc=34.63°
g4, φc=34.50°

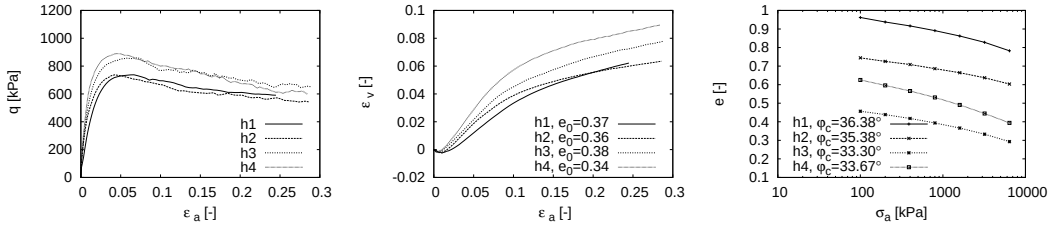
q [kPa]
ε a [-]
h1
h2
h3
h4
ε v [-]
h1, e0=0.37
h2, e0=0.36
h3, e0=0.38
h4, e0=0.34
e [-]
σa [kPa]
h1, φc=36.38°
h2, φc=35.38°
h3, φc=33.30°
h4, φc=33.67°

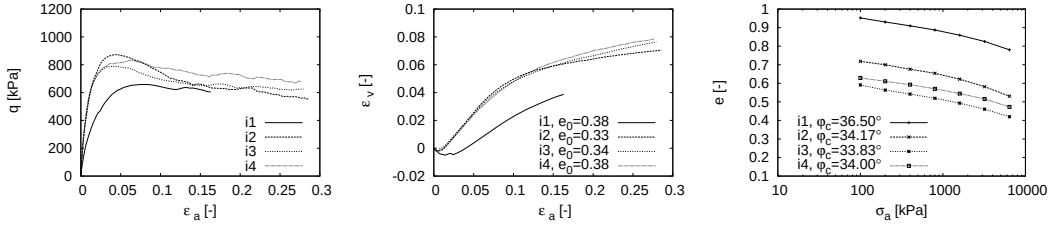
q [kPa]
ε a [-]
i1
i2
i3
i4
ε v [-]
i1, e0=0.38
i2, e0=0.33
i3, e0=0.34
i4, e0=0.38
e [-]
σa [kPa]
i1, φc=36.50°
i2, φc=34.17°
i3, φc=33.83°
i4, φc=34.00°

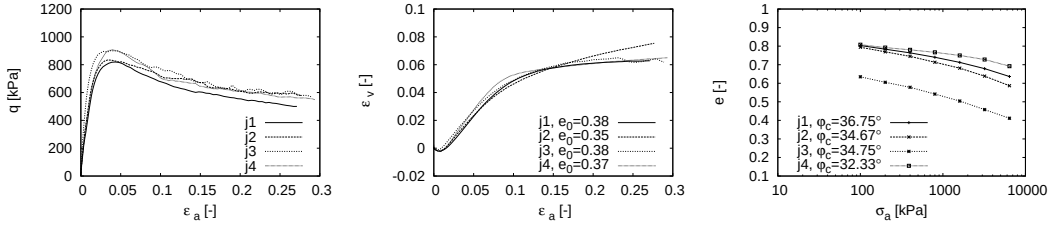
q [kPa]
ε a [-]
j1
j2
j3
j4
ε v [-]
j1, e0=0.38
j2, e0=0.35
j3, e0=0.38
j4, e0=0.37
e [-]
σa [kPa]
j1, φc=36.75°
j2, φc=34.67°
j3, φc=34.75°
j4, φc=32.33°